

Surface Modification of TiO_2 @Pvc Composite Membrane for Textiledye House (Brome Phenol Blue) Filtration

AbeerA.Emam¹, Mahmoud Fathy^{2*}, R.hoasny³ and Sanaa Naeim⁴

^{1,4}Faculty of Science, El-Azhar University, Cairo, Egypt

^{2,3}Egyptian Petroleum Research Institute (EPRI)

*Corresponding author

Mahmoud Fathy, Ahmed El-Zomer, Nasr City, Egyptian Petroleum Research Institute (EPRI), Box. No. 11727, Cairo, Egypt, Tel: + (202)22747847, Fax: + (202)22747433, E-Mail: Fathy8753@yahoo.com

Submitted: 19 Nov 2019; Accepted: 25 Nov 2019; Published: 20 Jan 2020

Abstract

The continued increase in the costs of chemicals, energy and water makes their recovery more important today than it was years ago when separation techniques by membrane filtration were first introduced to the textile industry. The aim of introducing membrane filtration is not only to reduce water consumption and wastewater streams. The paper describes the results of research works and implementation project concerning cleaner technology and water reuse in textile dye house by TiO_2 @PVC composite membrane. Fabricated membranes were characterized with various analytical and experimental techniques. Results showed that the TiO_2 blend TiO_2 @PVC composite membrane were nano porous in nature with improved porosity and permeability. Addition of TiO_2 improved the mechanical stability and water permeability of the composite membranes. TiO_2 doped membrane showed better dye rejection behavior with a permeate flux. Size and charge based exclusions along with adsorption were identified as the separating principles. Fouling analysis clearly showed that TiO_2 incorporated membranes possessed better antifouling effect than membrane without TiO_2 . Thus the TiO_2 blended TiO_2 @PVC composite membrane are promising for the treatment of dye polluted wastewater.

Keywords: Filtration, Membrane, Composites, Nanoparticles, Wastewater, Pollution

Introduction

Membrane filtration as a means of purification or concentration relies on the principle that when a liquid is passed across or through a physical barrier, particles whose size is larger than the pores in the membrane are retained on one side of the barrier, while the remaining liquid is allowed to pass through [1]. This principle holds true for coarse filters, such as metal sieves, as well as much finer materials which are capable of selective filtration and concentration of molecules of different sizes [2].

Over the past 15 years membrane filtration, which uses a polymer or similar material with an extremely small pore size, has become increasingly popular in industrial processes where reliable and repeatable purification or concentration are required [3]. The technology is now being applied widely in dye manufacturing and textile coloring [4]. This article sets out to explain how membrane filtration works and where it can be used successfully in the dye industry.

Ultrafiltration (UF), a separation technique characteristically placed between microfiltration (MF) and nanofiltration (NF), has received growing attention in the field of dye effluent treatment. MF has restricted applications since MF membranes with large pore sizes in

the 0.1–10 μm range fail to remove dye molecules with molecular weights ranging from a few hundred to over a thousand Daltons, whereas NF rejects effectively most dyes but faces a large energy requirement and serious membrane fouling issues [5,6]. UF can combine the advantages from both MF and NF to give satisfactory efficiency with much less energy consumption and is hence widely utilized for separating dyes [7].

Filters of any type serve two purposes. They retain some material and allow the remainder to flow through to the next stage in a process. When making a cup of tea using tea leaves, the strainer collects the leaves (known as the retentate or concentrate) and allows the liquid which has been flavored and colored by the leaves (the permeate or filtrate) to flow through [8]. Sometimes, as is the case when making tea, the retentate is an unwanted waste material and the permeate is the product of value. However, other applications rely on the efficient collection of the retentate. When panning for gold the prospector obviously wants to keep the small particles of metal but has no interest in the permeate water [9, 10].

The present work was aimed at fulfilling this gap in the literature by exploring the separation behaviors of dye mixtures across a TiO_2 @PVC composite membrane. Herein, four representative dyes with different charges were used for various binary dye solutions, including brome phenol blue. The membrane filtration performance for the dye feed solutions was investigated. The dye separation

mechanisms were proposed. Multi-cycle operation was performed to validate the reusability of the membrane.

Experimental and Materials

Membrane Synthesis

Non-solvent induced phase separation (NIPS) method was used to make membranes. Polymer dope solution was prepared by dissolving PVC in DMAc. Concentration of PVC was kept at 12% (by wt.) The value of concentration of PVC are chosen in such a way (based on the literature survey) that the prepared membrane are porous and their application lies in the ultrafiltration range. The casting solution was kept at 70°C, and magnetically stirred for 24 h to ensure homogeneity. Then, the solution was allowed to degas at room temperature overnight without stirring. Finally, the membrane was casted on the non-woven sheet using Automatic film applicator (Make: Sheen Instruments). The wet thickness was maintained up to 150 μm while casting. The casted membrane was immediately immersed into DI water bath (that act as non-solvent coagulation bath) for phase inversion, and kept under water for at least 24 h to ensure the removal of traces of solvent present in the membrane. Then, the membrane was dried at room temperature. All membranes were kept in DI water for few hours before use. TiO₂/PVC blend membrane were prepared by dispersing 0.5%, 1%, 1.5% and 2% TiO₂ nanoparticle composites in the solvent (DMAc), followed by addition of 12% PVC (all the percentages are on w/w basis). The optimized composition of the casting solution was selected based on the literature surveyed. The preparation of casting solution and membrane casting by phase inversion was done according to the aforementioned method.

Membrane Module TiO₂@PVC Composite Membrane and Experimental Procedure

The schematic of TiO₂@PVC composite membrane was used in the experiments is shown in Figure 1. For all experiments, we operated at constant Cross Flow Velocity (CFV=4 m/s). The permeate was not recycled in the feed tank [11].

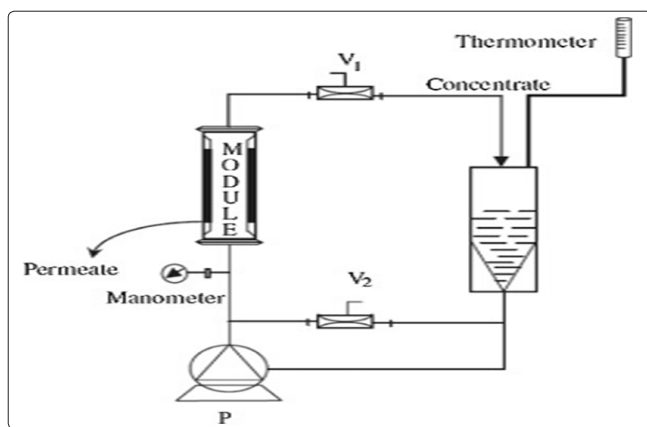


Figure 1: The schematic of TiO₂@PVC composite membrane

A membrane TiO₂@PVC composite membrane flat sheet was used to filter the colored solutions. The specifications of the membrane are given in Table 1.

Table 1: Ceramic membrane specifications

Membrane	T170-50n TZ
Type	Tubular
Active layer	TiO ₂ @PVC composite membrane
Nominal pore size	70 nm
Membrane	T170-50n TZ
Deionized water permeability	
Effective filtration area	50 cm ²
Maximum operating temperature	95 °C
Maximum operating pressure	10 bar
pH range	0–14

Experiments were carried out under three different temperatures (20, 30, and 40 °C) in order to observe membrane performances at each temperature. The process performances were studied in terms of both, permeate flux and permeate quality.

After each MF run, the membrane was subjected to a cleaning cycle which included in the first place a rinse with deionized water at 25 °C (15 min). Next, an alkaline cleaning with aqueous NaOH solution (pH 13) at 60 °C (1 h) took place.

Finally, the membrane was rinsed with deionized water until neutrality. The cleaning procedure after runs with the feed concentration included an additional step since alkaline cleaning was not enough to recover the initial permeability. It consisted of an acid cleaning step with the aqueous citric acid solution (pH 2) at 40 °C (1 h), followed by rinsing with deionized water until neutrality was reached.

All the cleaning steps, including rinses, were conducted at a CFV of 3 m/s and no pressure was applied. Once the membrane was cleaned, the water permeability was checked. The mentioned cleaning process allowed initial flux recoveries higher than 90%.

The permeate flux is calculated according to Eq. (1)

$$(1) J_p = \frac{V}{A \cdot t} \quad [12]$$

Where J_p is the permeate flux (L/m²h), V is the permeate volume (L), A is the effective membrane area (m²) and t is the sampling time (h). At the same time, permeate samples were collected for water quality analysis. The rejection coefficient (R) is calculated as a percentage according to Eq. (2)

$$(2) R\% = 1 - C_p/C_f \times 100$$

where C_f is the concentration in the feed stream and C_p is the concentration in the permeate stream [13].

The volume reduction factor (VRF) is equal to the initial feed volume divided by the retentate volume:

$$(3) VRF = \frac{V_f}{V_r} \quad [14]$$

Darcy's law is commonly used to determine filtration resistance in permeate transport through porous membranes according to Eq. (3)

$$(4) J_p = \frac{\Delta P}{\mu R_t}$$

where J_p is the permeate flux ($L h^{-1} m^{-2}$), ΔP is the transmembrane pressure (Pa); μ is the dynamic viscosity of the feed (Pa s) and R_t is the total filtration resistance (m^{-1}) [15].

Resistances in series models of fouling often subdivide the total membrane resistance R_t into three components, namely intrinsic membrane resistance R_m , external (concentration polarization) resistance R_{cp} ; and internal resistance R_f , due to fouling.

Characterization of $TiO_2@Pvc$ Composite Membrane

The characterization methods of chemical composition, crystalline phase composition (XRD) and Thermo-gravimetric analysis (TGA/DTG) were already explained in a previous work. The surface morphology, the presence of possible defects and the pore structure of the sintered MF membranes were analyzed by Scanning Electron Microscopy (SEM) (Hitachi, S-4500). The apparent porosity, water adsorption and apparent density were measured in accordance with ASTM C373-88 method using distilled water as an immersion medium.

Results and Discussion

Microstructure

The micrographs of MF membranes prepared with (0-20 wt.%) of corn starch are shown in Fig. 4a–e, the micrographs indicate that the effect of corn starch content on the microstructure of MF membranes is very remarkable. The addition of starch by more than 10 wt.% produced MF membranes with more and bigger pores which lead to more porous structure. An increasing of the connectivity between pores can be seen as dark areas in the image (Fig. 4).

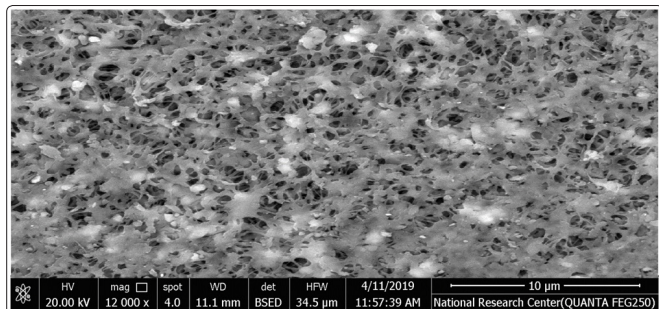


Figure 2

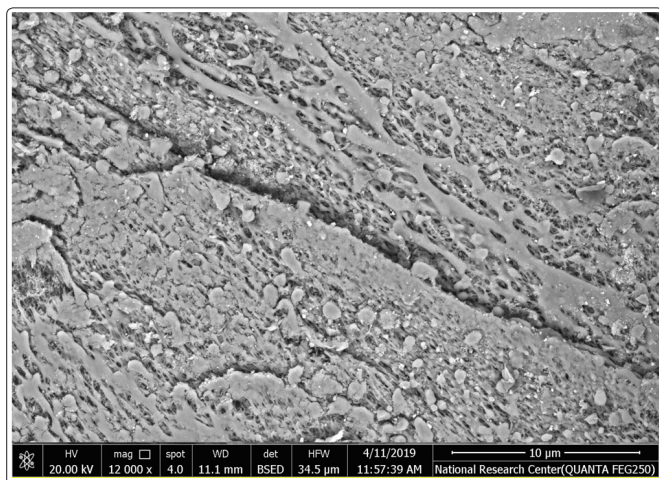


Figure 3

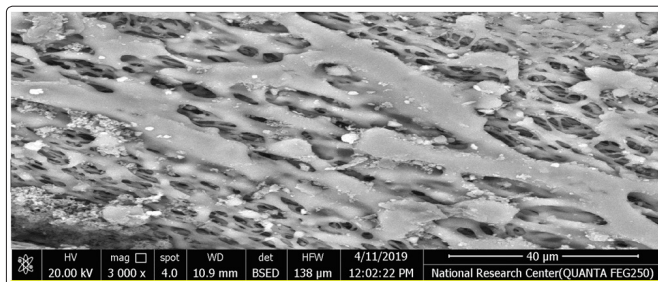


Figure 4: SEM images of MF membranes elaborated with: (a) PVC; (b) 15 wt. %/ TiO_2 /PVC; (c) composite membrane with dye

Scanning electron microscopy (SEM) was applied to investigate the surface and cross sectional morphology of the prepared membranes using VEGA\TESCAN SEM, Czech Republic. For cross-sectional images. The membranes were fractured in liquid nitrogen. The samples were coated with gold before SEM analysis. In addition since SEM device was equipped with dispersive X-ray analysis (EDAX) detector, this analysis was used to inspect dispersion of nano- TiO_2 particles in the cross section of the fabricated membranes.

FTIR of Prepared Compounds

Fourier-Transform Infrared (FTIR) Spectroscopy

FTIR spectroscopy is a vibrational spectroscopy that records absorptions of IR light by chemical bonds in all molecules including polymers. Since different bonds absorb IR light at different wavelengths, FTIR spectroscopy is often referred to as fingerprint spectroscopy. As a consequence pure compounds have characteristic and unique FTIR spectra. Scanning was carried out from 4000 cm^{-1} ($2.5\text{ }\mu\text{m}$) to 500 cm^{-1} ($20\text{ }\mu\text{m}$) to confirm the formation of the graft copolymerization with FTIR-spectrophotometer (Shimadzu-IRTracer-100, Japan) at the Chemistry Department, Al-Mustansiriyah University, Iraq.

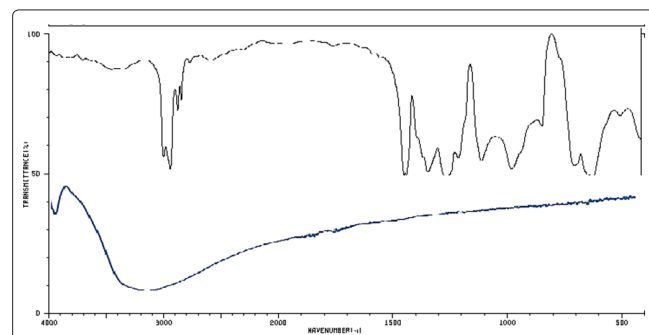


Figure 5: FTIR of TiO_2 and composite membrane

Membrane Performance Test

Analysis of Resistances

Fig 6 illustrates the membrane fouling of ultrafiltration in treating textile wastewater at $CFV = 6\text{ m/s}$ and $TMP = 2.05\text{ bar}$ with different temperatures 20, 30 and $40\text{ }^\circ\text{C}$. R_m decreases with increasing temperature, due to lower values of the viscosity of the liquid, and because of the increase of the mass-transfer coefficient according to the film model, both effects providing higher pure water permeate flux at higher temperature. On the contrary, R_a increases with temperature, indicating more severe fouling phenomena at the higher temperature [16]. As consequence, a temperature increase results first in a greater external fouling on the membrane surface probably due to an increment of the internal fouling due to adsorption and

pore blocking. As filtration times progress, the adsorption resistance (R_a) increased. This increase due to high turbulence (CFV = 6 m/s) can cause the relatively smaller or finer particles. The finer particles present in textile wastewater are then deposited either in the membrane pore opening or into membrane pores channels [17].

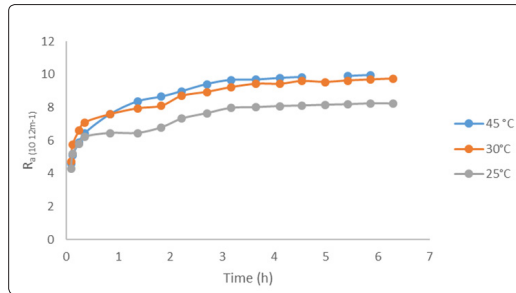


Figure 6: Evolution of the intrinsic resistance and adsorption resistance with time at different temperatures (CFV=6 m/s, TMP=2.05 bar)

Effect of Temperature

From the relation between VRF and filtration time, it is easy to deduce the influence of VRF for the experiments. Fig. 7 shows the effect of temperature on permeate flux decline, the flux increases with VRF increases, due to increasing fouling [18]. Moreover, these curves could be divided into three periods: an initial stage with a rapid decrease of the permeate flux; a second stage with a smaller decrease of the permeate flux that takes place around VRF=1.25 and a final stage with observed a constant flux after VRF=1.25.

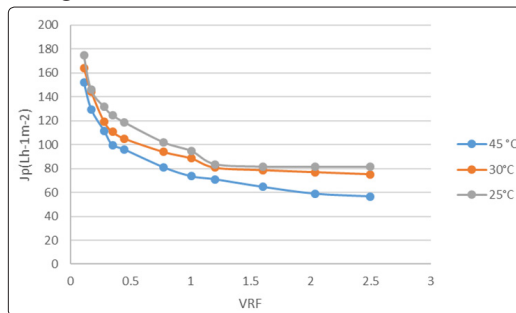


Figure 7: Evolution of the permeate flux with the volume retention factor (CFV=6 m/s, TMP=2.05 bar)

The results obtained during experiments with textile wastewater showed that permeate flux decline from the beginning of the run to the steady-state condition was lower at the higher temperature (Fig 4). In fact, as an example, for a fixed TMP of 4 bar, permeate flux decreased by 80.5% from its initial value when the operating temperature was set at 20°C. Lower permeate flux decline as temperature increases is a consequence of the reduction of membrane fouling and concentration polarization under higher temperature [19].

The temperature of textile wastewater was controlled from 20 to 40°C using a water bath. Fig.5 Shows the variation of the permeate flux after 6h of filtration at different feed temperatures. The permeate flux increases by 18% with increases of feed temperature from 20 to 40°C. As seen, at a higher temperature cake layer formation is limited and permeate flux is almost constant. It must be mentioned that by increasing temperature, permeate flux increases. Temperature has double effects on permeation flux; increasing temperature decreases viscosity, and as a result increases permeation flux. From another

point of view, increasing temperature increases osmotic pressure and this decreases permeation flux [20]. Therefore, because of the bilateral effects of temperature must be specified. Higher feed temperature leads to lower viscosity of feed and also higher solubility of some feed constituents. The same reduces concentration polarization and transport of solvent through the membrane intensifies, yielding a higher permeates flux. It should be noted that the elevation of feed temperature normally increases the energy cost and the potential of scaling, and reduces the durability of the membrane system in spite of superior thermal stability of ceramic membrane compared to the polymeric membrane [17].

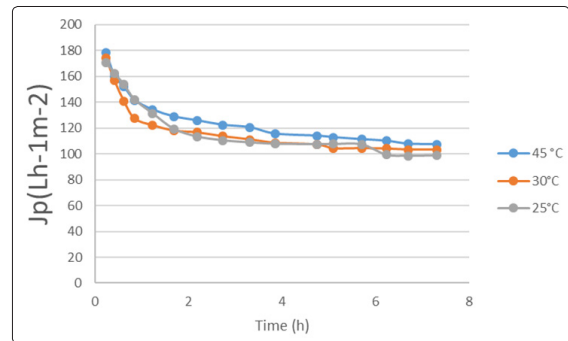


Figure 8: Effect of temperature on permeate flux (CFV=6 m/s, TMP=2.05 bar)

The collected permeate under a TMP of 2.05 bar was used as feed for all the ED system. This pre-treatment step was obtained a clear permeate by removing organic matters.

The cumulative permeate volume V_p obtained as a function of time for the ceramic membrane at different temperature and with constant CFV = 6 m/s, is represented in Fig. 9. As it can be observed, these volumes increased with processing time, but simultaneously, a decrease occurred in the permeate rate. Additionally, for a given time, the volumes decreased with increased temperature. Fig. 9 also includes the cumulative permeate volume obtained in the previous experiments for the filtration of pure water with the ceramic membrane [21]. The lower values of V_p obtained of textile wastewater in comparison to those of pure water were due to the fouling of the membrane. It is also seen that there is a linear relationship between the permeate volume of pure water and time, which implies that J_p is constant. This is in accordance to the resistance in the series model, given by Darcy's law.

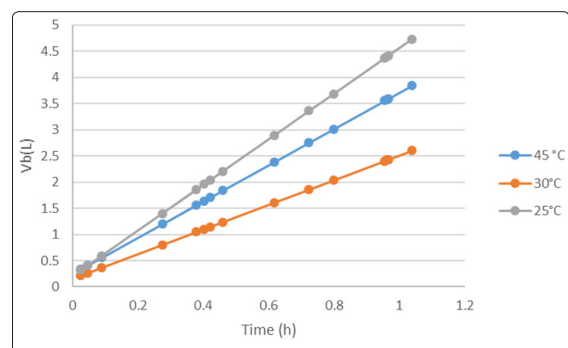


Figure 9: Evolution of the cumulative permeate volume with processing time for the wastewater filtration with the ceramic membrane at a tangential velocity CFV=6 m/s

Conclusion

Due to the special properties of TiO₂ nanoparticles and PVC polymer, TiO₂ embedded PVC membranes were prepared via non solvent induced phase separation method. The results from this study showed that TiO₂ nanoparticles could be dispersed uniformly within the PVC membranes at 0.5, 1.0, 1.5, 2 wt.% TiO₂ embedded PVC membranes. Even though hydrophilicity, pure water flux and antifouling properties of TiO₂ embedded membranes were higher than those of neat PVC membrane, the rejection of composite membranes reduced due to the increase in mean pore radius. However, flux decline of PVC/TiO₂ membranes were significantly lower than that of neat PVC membrane. It was concluded that incorporation of TiO₂ nanoparticles improved fouling resistance of PVC/TiO₂ membranes

There is no conflict of interest for that paper.

References

1. Homem NC, Natálide Camargo Lima Beluci, Sara Amorim, Rui Reis, Angélica Marquetotti Salcedo Vieira et al. (2019) Surface modification of a polyethersulfone microfiltration membrane with graphene oxide for reactive dyes removal. *Applied Surface Science* 486: 499-507.
2. Yan Z, Haiyang Yang, Fangshu Qu, Han Zhang, Hongwei Rong et al. (2019) Application of membrane distillation to anaerobic digestion effluent treatment: Identifying culprits of membrane fouling and scaling. *Science of The Total Environment* 688: 880-889.
3. Anuj SA, Gajera HP, Hirpara DG, Golakiya BA (2019) Bacterial membrane destabilization with cationic particles of nano-silver to combat efflux-mediated antibiotic resistance in Gram-negative bacteria. *Life Sciences* 230: 178-187.
4. Zheng L, Dawei Yu, Gang Wang, Zenggang Yue, Chun Zhang et al. (2018) Characteristics and formation mechanism of membrane fouling in a full-scale RO wastewater reclamation process: Membrane autopsy and fouling characterization. *Journal of Membrane Science* 563: 843-856.
5. Tian J, Meilan Pan, Yunqiao Ma, Jia Wei Chew (2019) Effect of membrane fouling on chiral separation. *Journal of Membrane Science* 593: 117352.
6. Bagbi Y, Pandey A, Solanki PR (2019) Chapter 10 - Electrospun Nanofibrous Filtration Membranes for Heavy Metals and Dye Removal. *Nanoscale Materials in Water Purification* Elsevier 275-288.
7. Zarei F, Rozita M. Moattari, Saeid Rajabzadeh, Maryam Bagheri, Abolfazl Taghizadeh et al. (2019) Preparation of thin film composite nano-filtration membranes for brackish water softening based on the reaction between functionalized UF membranes and polyethyleneimine. *Journal of Membrane Science* 588: 117207.
8. Liu C, Jing-ying Xu, Jun-feng Qi, Yan-jie Liu, Jia-wei Kang et al. (2019) A novel nanobiocomposite sandwich immunosensor based on molecularly imprinted nano-membrane for endotoxin detection. *Sensors and Actuators B: Chemical* 290: 1-8.
9. Abo-Elmaged H H, Gaber AA (2017) Synthesis and characterization of nano-hydroxyapatite membranes for water desalination. *Materials Today Communication* 13: 186-191.
10. Li Q, Zhipeng Liao, Xiao feng Fang, Dapeng Wang, Jia Xie et al. (2019) Tannic acid-polyethyleneimine crosslinked loose nanofiltration membrane for dye/salt mixture separation. *Journal of Membrane Science* 584: 324-332.
11. Deng N, Hongsheng He, Jing Yan, Yixia Zhao, Eya Ben Tich et al. (2019) One-step melt-blowing of multi-scale micro/nano fabric membrane for advanced air-filtration. *Polymer* 165: 174-179.
12. Nam YH, eung-Ki Lee, Jong-Ho Kim, Jae-Hyoung Park (2019) PDMS membrane filter with nano-slit array fabricated using three-dimensional silicon mold for the concentration of particles with bacterial size range. *Microelectronic Engineering* 215: 111008.
13. Dlamini DS, Mamba BB, Li J (2019) The role of nanoparticles in the performance of nano-enabled composite membranes – A critical scientific perspective. *Science of The Total Environment* 656: 723-731.
14. Wang Z, Tang Y, Wang T, Liang K (2019) Nano CuAl₂O₄ spinel mineral as a novel antibacterial agent for PVDF membrane modification with minimized copper leachability. *Journal of Hazardous Materials* 368: 421-428.
15. Li J, Gong JL, Zeng GM, Zhang P, Song B et al. (2019) The performance of UiO-66-NH₂/graphene oxide (GO) composite membrane for removal of differently charged mixed dyes. *Chemosphere* 237: 124517.
16. Nikooe N, Saljoughi E (2017) Preparation and characterization of novel PVDF nanofiltration membranes with hydrophilic property for filtration of dye aqueous solution. *Applied Surface Science* 413: 41-49.
17. Liu D, Zhu Z, Zhao Y, Chen Y, Tan Y et al. (2019) Low pressure modified polyamide 6 membrane for effective fractionation of dyes and NaCl. *Science of The Total Environment* 695: 133908.
18. Soyekwo F, Changkun Liu, Hao Wen, Yunxia Hu (2019) Construction of an Electron Neutral Zinc Incorporated Polymer Network Nanocomposite Membrane with Enhanced Selectivity for Salt/Dye Separation. *Chemical Engineering Journal* p. 122560.
19. Ouaddari H, Karim A, Achiou B, Saja S, Aaddane A et al. (2019) New low-cost ultrafiltration membrane made from purified natural clays for direct Red 80 dye removal. *Journal of Environmental Chemical Engineering* 7: 103268.
20. Liu Y, Weiya Zhu, Kang Guan, Cheng Peng, Jianqing Wu (2018) Freeze-casting of alumina ultra-filtration membranes with good performance for anionic dye separation. *Ceramics International* 44: 11901-11904.
21. Zhao S, Wang Z (2017) A loose nano-filtration membrane prepared by coating HPAN UF membrane with modified PEI for dye reuse and desalination. *Journal of Membrane Science* 524: 214-224.

Copyright: ©2020 Mahmoud Fathy. This is an open-access article distributed under the terms of the Creative Commons Attribution License, which permits unrestricted use, distribution, and reproduction in any medium, provided the original author and source are credited.